JOURNAL OF VIROLOGY, July 1993, p. 4037–4049
0022-538X/93/074037-13$02.00/0

Vol. 67, No. 7

Purification and Characterization of an Active Human Immunodeficiency Virus Type 1 RNase H Domain

JEFFREY S. SMITH AND MONICA J. ROTH*

Department of Biochemistry, Robert Wood Johnson Medical School, University of Medicine and Dentistry of New Jersey, 675 Hoes Lane, Piscataway, New Jersey 08854-5635

Received 11 December 1992/Accepted 5 April 1993

We have expressed and purified from *Escherichia coli* a human immunodeficiency virus type 1 (HIV-1) RNase H domain consisting of amino acids 400 to 560 of reverse transcriptase with either an N- or C-terminal polyhistidine tag. The native protease cleavage site of HIV-1 reverse transcriptase is between amino acids 440 and 441. Purification on Ni^{2+}-nitrilotriacetate agarose resulted in a highly active RNase H domain dependent on $MnCl_2$ rather than $MgCl_2$. Activity was unambiguously attributed to the purified proteins by an in situ RNase H gel assay. Residues 400 to 426, which include a stretch of tryptophans, did not contribute to RNase H activity, and the polyhistidine tag was essential for activity. Despite the requirement for a histidine tag, the recombinant RNase H proteins retained characteristics of the wild-type heterodimer, as determined by examining activity in the presence of several known inhibitors of HIV-1 RNase H, including ribonucleoside vanadyl complexes, dAMP, and a monoclonal antibody. Importantly, the isolated RNase H domain produced the same specific cleavage in $tRNA_3^{Lys}$ removal as HIV-1 heterodimer, leaving the 3′-rA (adenosine 5′ phosphate) residue of a model tRNA attached to the adjacent U5 sequence. This HIV-1 RNase H domain sedimented as a monomer in a glycerol gradient.

The reverse transcriptase (RT) of human immunodeficiency virus type 1 (HIV-1) is responsible for the conversion of its single-stranded RNA genome into double-stranded DNA. The enzyme is multifunctional, with both RNA- and DNA-dependent DNA polymerase and RNase H activities (for reviews, see references 7, 54–56). Recently, a double-stranded RNase activity has also been reported to be associated with RT and termed RNase D (3, 4). RNase H activity is required during reverse transcription to degrade the viral RNA template, as well as to remove the plus-strand polypurine tract RNA primer and minus-strand $tRNA_3^{Lys}$ primer. The removal of $tRNA_3^{Lys}$ is accomplished through a specific endonucleolytic cleavage event 5′ of the terminal rA (adenosine 5′ phosphate) of the 5′-CCA-3′, resulting in a ribonucleotide being present at the U5 terminus of the double-stranded DNA (12, 39, 48).

HIV-1 RT is a heterodimer composed of p66 and p51 subunits (9, 30). The p51 subunit is a C-terminal-truncated version of p66. p51 is produced through the action of the viral-encoded protease that cleaves the p66 subunit between positions 440 and 441 of the amino acid sequence (33). The polymerase activity of RT has been localized to the N terminus of p66, while the RNase H domain has been localized to the C terminus. Deletion, linker insertion, and cassette mutagenesis studies, however, have shown a high level of interdependence between the two domains (5, 17, 38); mutations in the polymerase domain can affect the RNase H domain, and vice versa. The DNA polymerase and RNase H active sites have been shown biochemically to be separated by a distance corresponding to approximately 15 to 18 bp (13, 15, 58) and to share the same template-primer binding site (PBS) (27). Structural data from crystallographic studies have confirmed these findings (1, 25).

Specific removal of the minus-strand $tRNA_3^{Lys}$ primer is observed in both the absence (39, 48) and the presence (12) of DNA polymerization. Two classes of RNase H activity, polymerase dependent and polymerase independent, have been observed (13). In the polymerase-dependent mode, the RNase H active site is believed to trail behind the polymerase active site. Removal of the $tRNA_3^{Lys}$ primer would be directed by the polymerase active site bound to the 3′ terminus of the plus strand currently being extended, thus positioning the RNase H domain over the RNA-DNA junction. Since this specific cleavage is also observed in the absence of DNA polymerization, an additional RNase H-binding mode and structural aspects of the U5–primer-binding site junction may also be responsible for specificity. What actually directs the RNase H specificity in removal of the $tRNA_3^{Lys}$ minus-strand primer remains to be determined.

The recombinant HIV-1 RNase H domain expressed and purified from *Escherichia coli* has been crystallized, and the structure has been determined (8). The N terminus of this RNase H was Tyr-427 rather than the natural protease cleavage site at position 441. The structure of this HIV-1 RNase H domain is similar to that of *E. coli* RNase H (24, 60). A major difference between the two is that the "handle" region of *E. coli* RNase H, consisting of α-helix C and a following loop (60), is missing in the corresponding region of HIV-1 RNase H (8). It is believed that this lysine-rich handle plays a major role in substrate binding (23). Also, in the HIV structure, a loop containing the conserved histidine-539 is disordered. Interestingly, the protein was inactive except when it was supplemented with a recombinant p51 domain (21). This suggests a dependence of RNase H activity on p51.

Several other investigators have expressed and purified similar recombinant HIV-1 RNase H domains, which either were inactive or showed extremely low levels of activity (2, 42, 49). In contrast, p15 RNase H immunoaffinity purified from virions (16) and a recombinant HIV-1 RNase H p15 domain bacterially expressed and purified by immobilized-metal affinity chromatography (IMAC) have been reported to be active (11). This RNase H was identical to the protein

* Corresponding author.

that was crystallized except that it had an IMAC-specific N-terminal extension of 12 amino acids that contained four histidine residues.

In the region of amino acids 398 to 426, a series of tryptophan residues have been proposed in a crystallographic study (8) to play a role in RNA-DNA hybrid binding. This proposal is based on the fact that there is also a tryptophan-rich domain in *E. coli* RNase H encompassing α-helices C and D as well as β-strand 5. To determine whether p51 residues upstream of the RNase H domain, including the tryptophan-rich region, play a role in RNase H activity, as well as in the specificity of $tRNA_3^{Lys}$ removal, we have expressed and purified from *E. coli* various recombinant HIV-1 RNase H domains and have characterized their enzymatic activity.

MATERIALS AND METHODS

Materials. Restriction enzymes, Vent DNA polymerase, and T4 DNA polymerase were purchased from New England Biolabs. T4 DNA ligase, T7 RNA polymerase, and *E. coli* RNase H were purchased from GIBCO-Bethesda Research Laboratories. Sequenase 2.0 was purchased from United States Biochemical Corp. *E. coli* RNA polymerase, T3 RNA polymerase, and recombinant RNasin were purchased from Promega. Highly purified recombinant HIV-1 RT was obtained from Jeffrey Culp, Department of Protein Biochemistry, SmithKline Beecham Pharmaceuticals. This recombinant HIV-1 RT consists of a p66-p51 heterodimer and was expressed in *E. coli* by in vivo processing of a *pol* precursor protein by HIV-1 protease produced in *trans*. This protein is similar, if not identical, in primary structure and function to the genuine viral enzyme (32). The purified p51 subunit of HIV-1 RT was provided by Stuart Le Grice (Case Western University). Purified *E. coli* RNase III (31) and an RNase III-specific polyclonal antibody were both provided by Paul March (University of Medicine and Dentistry of New Jersey). [α-^{32}P]CTP, α-^{35}S-dATP, and [α-^{32}P]dATP were obtained from Amersham. [5,6-^{3}H]UTP was from New England Nuclear. The ribonucleoside vandyl complex (RVC) and thrombin were purchased from Sigma.

Expression vector construction. A DNA fragment corresponding to amino acids 400 to 560 of HIV-1 RT (HXB2 sequence) was produced by a polymerase chain reaction (PCR) with the plasmid pRT4, which encodes the RT gene (provided by Brad Preston) as the template, 34-mer oligonucleotide 3555 (5′-CGGATCCTACAATATTTTCCTGATTC CAGCACTG-3′) as the C-terminal-specific primer, and 30-mer 3556 (5′-GCATATGCATACATGGTGGACAGAGTAT TG-3′) as the N-terminal-specific primer. DNA amplification was performed with Vent DNA polymerase by using the standard reaction conditions recommended by New England Biolabs. The reaction included 1 ng of pRT4 template DNA linearized with *Hin*dIII and 50 pmol each of primer 3555 and 3556. Because the 5′ end of each primer contained noncomplementary restriction site sequences, hybridization was performed at 50°C for the first 5 cycles and at 58°C for the remaining 25 cycles. The resulting 502-bp product was inserted into the *Sma*I site of pTZ18U (United States Biochemical Corp.). Oligonucleotides 3554 (5′-GGTGATGG TGATGGTGATGCA-3′) and 3557 (5′-TCACCATCACCAT CACCTGCA-3′), together consisting of the N-terminal histidine tag, were annealed and ligated into the N-terminal *Nsi*I site encoded in the 5′ end of primer 3556. To construct the C-terminal histidine-tagged coding sequence, oligonucleotides 2842 (5′-ACATCACCATCACCATCACTAGTA-3′) and 2843 (5′-TACTAGTGATGGTGATGGTGATGT-3′), together consisting of the C-terminal His tag, were annealed and ligated into the *Ssp*I site created at the C terminus of the RNase H PCR product. An *Nde*I-*Bam*HI fragment was then excised and inserted into the *Nde*I-*Bam*HI sites of pET-11c (Novagen) to produce either pET-RHN2 or pET-RHC1.

A thrombin protease cleavage site was inserted between the histidine tag and RNase H sequences by construction of the vector pET-RHN2T. To construct this vector, a *Nde*I-*Bam*HI PCR fragment without a histidine tag was inserted into the corresponding sites of the vector 6HisT-pET11 (19).

A DNA fragment corresponding to amino acids 427 to 510 was amplified with the oligonucleotide primers 4113 (5′-GCATATGTACCAGTTAGAGAAAGAACC-3′) and 4115 (5′-CTGGTTGTGCTTGAATGATTCC-3′) and ligated into the *Sma*I site of pTZ18U. A *Nde*I-*Nsi*I fragment was then excised and ligated as a cassette into either pET-RHC1 or pET-RHN2T predigested with *Nde*I and *Nsi*I to produce the expression vector pET-CY427 or PET-NY427, respectively.

The reading frames of all constructs were verified by DNA sequencing. pET-RHN2, pET-RHC1, and pET-RHN2T were transformed into *E. coli* HMS174DE3 and upon induction produced the recombinant HIV-1 RNase H proteins RHN-2, RHC-1, and RHN-2T, respectively. pET-CY427 and pET-NY427 were transformed into strain BL21DE3 and upon induction produced the recombinant RNase H domains CY427 and NY427.

Protein purification. Purification was performed as described previously for Moloney murine leukemia virus (Mo-MuLV) integrase (22), with several modifications. pET-RHN2, pET-RHC1, and pET-RHN2T were expressed in HMS174DE3 cells, while pET-NY427 and pET-CY427 were expressed in BL21DE3 cells. Induction of the starting vector pET11c was followed by parallel purification, as a control for contaminating proteins. Cultures (750 ml) of the appropriate *E. coli* strain containing one of the expression vectors were grown at 37°C to an optical density at 600 nm of 0.8 and then induced by the addition of isopropyl-β-D-thiogalactopyranoside (IPTG) to 1 mM. After an additional 3 h of growth at 37°C, the cells were pelleted and then solubilized in 50 ml of buffer A (10 mM Tris base, 0.1 M Na_2HPO_4, 0.1% Nonidet P-40, 10 mM β-mercaptoethanol, 100 mM NaCl, 10% glycerol, 4 M urea [pH 8.0]) with slow shaking for 1 h at room temperature. The slurry was centrifuged at 8,000 × *g* at 4°C for 25 min, and the supernatant was applied to a 1-ml nickel nitrilotriacetate (NTA) affinity column pre-equilibrated with buffer A (pH 8.0) at 4°C. The column was then washed with 10 column volumes each of buffer A at pH 8.0, 6.3, 5.9, and 4.5. Fractions (1 ml) were collected for each pH step. HIV-1 RNase H peak fractions from the pH 4.5 wash were pooled, dialyzed overnight in 1 liter of buffer B (50 mM Tris-HCl [pH 8.0], 50 mM KCl, 2 mM dithiothreitol [DTT], 1 mM EDTA, 0.6% Triton X-100, 20% glycerol, 4 M urea), and reapplied to the column. Another series of step pH washes were performed with buffer A, and 1-ml fractions were again collected. Fractions were slowly renatured by step dialysis from 3 to 0 M urea in buffer B over 4 days and then stored at −80°C in 50% glycerol–buffer B.

pET-NY427 was also purified as a soluble protein essentially as described by Evans et al. (11), with a few modifications. Induction with IPTG was the same as for the denaturing conditions. Cells were disrupted by a French pressure apparatus in equilibration buffer (20 mM Tris-HCl, pH 8.0) containing 1 mM phenylmethylsulfonyl fluoride, 2 μg of leupeptin per ml, 2 μg of aprotinin per ml, and 1 mM benzamidine and then centrifuged at 8,000 × *g* for 1 h at 4°C.

The supernatant was passed through a 1-ml NTA column equilibrated with 20 mM Tris-HCl, pH 8.0. The column was washed sequentially with 10 column volumes of each of the following buffers: (i) equilibration buffer plus 1 M NaCl, (ii) equilibration buffer, (iii) equilibration buffer plus 25 mM imidazole, and (iv) equilibration buffer plus 30 mM imidazole. The column was then eluted with a 10-ml 20 to 60 mM imidazole gradient. Finally, the expressed protein was eluted off the column with 10 ml of equilibration buffer plus 100 mM imidazole. Fractions (1 ml) were collected and individually dialyzed against buffer B.

The various protein fractions were analyzed by sodium dodecyl sulfate (SDS)–17.5% polyacrylamide electrophoresis and Coomassie staining. Western immunoblot analysis was performed by using RT-specific monoclonal antibody (MAb) 15 (provided as a gift by Tobias Restle [43]). The protein concentration was determined by using the method of Bradford (6).

Thrombin cleavage assay. Removal of the N-terminal histidine tag was accomplished by incubating 50 μg of RHN-2T in a 300-μl reaction mixture containing 50 mM Tris-HCl (pH 8.0), 150 mM KCl, 2.5 mM $CaCl_2$, 17% glycerol, and 2.8 μg of thrombin per ml for 1.5 h at 25°C. A 50% slurry (100 μl) of Ni^{2+}-NTA resin was then added and bound for 30 min at 4°C. Following centrifugation for 0.5 min at 12,000 × *g*, the supernatant was removed, and the protein was then analyzed by SDS-polyacrylamide gel electrophoresis (PAGE) and RNase H assays.

Nonspecific RNase H assay. The RNA-DNA hybrid was prepared as previously described (44) by using circular single-stranded phagemid DNA as a template for *E. coli* RNA polymerase and [^{3}H]UTP (37.5 Ci/mmol) as the label. RNase H reaction mixtures (50 μl) under the indicated buffer conditions and containing 3 pmol of substrate were incubated at 37°C for 30 min. The reactions were stopped by the addition of 50 μl of 100 mM $NaPP_i$ (pH 6), followed by precipitation with trichloroacetic acid (TCA). The mixture was centrifuged for 10 min, and the radioactivity of the supernatant was determined with a liquid scintillation counter. In the case of the inhibitor studies, 1 pmol of each RNase H was preincubated with inhibitor for 10 min on ice prior to the addition of the substrate. Reaction mixtures were incubated for 4 min at 37°C.

In situ gel assay. The RNA-DNA hybrid substrate was prepared by using [α-^{32}P]CTP as described for the [^{3}H]UTP-labeled substrate. Protein samples were separated on an SDS–17% polyacrylamide gel that was copolymerized with 6 × 10^6 cpm of the [α-^{32}P]CTP-labeled substrate. The gel was then soaked in a buffer containing 50 mM Tris-HCl (pH 8.0), 50 mM KCl, 8 mM $MnCl_2$ or $MgCl_2$, and 2 mM DTT, with slow shaking at room temperature. The buffer was changed once every 24 h for at least 3 days. The gel was then directly exposed to X-ray film and stained with Coomassie brilliant blue.

Minus-strand primer removal assay. The substrate for determining the site of HIV-1 RNase H cleavage in the removal of a model $tRNA_3^{Lys}$ minus-strand primer was produced as previously described (48). The DNA portion of this substrate was labeled with [α-^{32}P]dATP. The RNA oligonucleotide (10 pmol; HPR-1) was annealed to 100 ng of single-stranded pMR2S-1 DNA and extended with T4 DNA polymerase in the presence of the restriction enzyme *Sma*I, which produces a product of a specific size that can be detected on a sequencing gel. The site of cleavage on the [α-^{32}P]dATP-labeled substrate was determined by incubating approximately 20 fmol of the RNA-DNA hybrid in a 20-μl reaction mixture with a final concentration of 20 mM Tris-HCl (pH 8.0), 8 mM $MnCl_2$, 2 mM DTT, and an indicated amount of purified HIV-1 RNase H domain or p51 polymerase subunit (provided by Stuart Le Grice). The reaction products were separated on a 10% sequencing gel and detected by autoradiography.

dsRNA-dependent RNase activity assay. In vitro transcription reactions were performed with pBluescriptII SK(+) as a DNA template and contained 40 mM Tris-HCl (pH 8.0), 25 mM NaCl, 8 mM $MgCl_2$, 2 mM spermidine, 62.5 μCi of [α-^{32}P]CTP (800 Ci/mmol), 0.5 mM (each) UTP, ATP, and GTP, 12 μM CTP, 3 μg of pBluescriptII SK(+), and either T7 (10 U) or T3 (10 U) RNA polymerase in a 20-μl reaction mixture. Reactions proceeded for 1 h at 37°C, and the mixture was then incubated with DNase I (2 μg) for 15 min at 37°C. The reaction mixtures were then extracted with phenol-chloroform and ethanol precipitated. Pellets were resuspended in 25 μl of 50% formamide, 300 mM NaCl, 50 mM sodium acetate (pH 4.8). The T7 and T3 transcripts were then mixed and annealed by incubation at 85°C for 5 min and then at 47°C for 1 h. The remaining single-stranded RNA was digested by incubation with 5 μg of RNase A for 1 h at 25°C, followed by digestion with proteinase K. The annealed substrate was extracted with phenol-chloroform and ethanol precipitated, and the pellet was resuspended in RNase-free water. The assay for double-stranded RNA (dsRNA)-dependent RNase activity was identical to the RNase H assay except that the dsRNA substrate was substituted for the RNA-DNA hybrid. To denature either the dsRNA or RNA-DNA hybrid, the substrates were heated to 90°C for 10 min and immediately transferred to dry ice. Reaction components were then added.

Glycerol gradient centrifugation. Purified RHN-2 or RHC-1 was layered onto a 10 to 30% glycerol gradient (4.75 ml) in a buffer containing 50 mM Tris-HCl (pH 8.0), 50 mM KCl, 2 mM DTT, 0.01% Triton X-100, and 0.1 mM EDTA. Aldolase (Sigma), Mo-MuLV RT (44), TFIIB (provided by D. Reinberg, (University of Medicine and Dentistry of New Jersey), and cytochrome *c* (Sigma) were layered onto a parallel gradient as sedimentation standards. The gradients were centrifuged at 48,000 rpm in a Sorvall AH-650 rotor at 4°C for 24 h. Fractions (125 μl) were collected from the bottom of the tube and assayed for RNase H activity by using the ^{3}H-labeled substrate under optimal RHN-2 buffer conditions. The markers aldolase and Mo-MuLV RT were assayed for activity (44), cytochrome *c* was detected by spectrophotometry (A_{295}), and TFIIB was detected by Western blot with a polyclonal TFIIB antiserum provided by Danny Reinberg.

RESULTS

Expression and purification of the HIV-1 RNase H domain. A portion of the HIV-1 RT gene encoding amino acids 400 to 560 (nucleotides 3746 to 4228 [40], HXB2 sequence) was amplified from the vector pRT4 by PCR. To facilitate purification of the subsequently expressed proteins, a tag of six histidine residues (18) was added to either the N or C terminus by insertion of an oligonucleotide linker into restriction sites added onto the N (*Nsi*I) or C (*Ssp*I) terminus of the PCR product. The resulting N- or C-tagged recombinant RNase H-coding fragments were subcloned into the *Nde*I and *Bam*HI sites of the expression vector pET11c (Novagen), downstream of the T7 RNA polymerase promoter, producing the RNase H expression vectors pET-RHN2 and pET-RHC1, respectively. The vector pET-

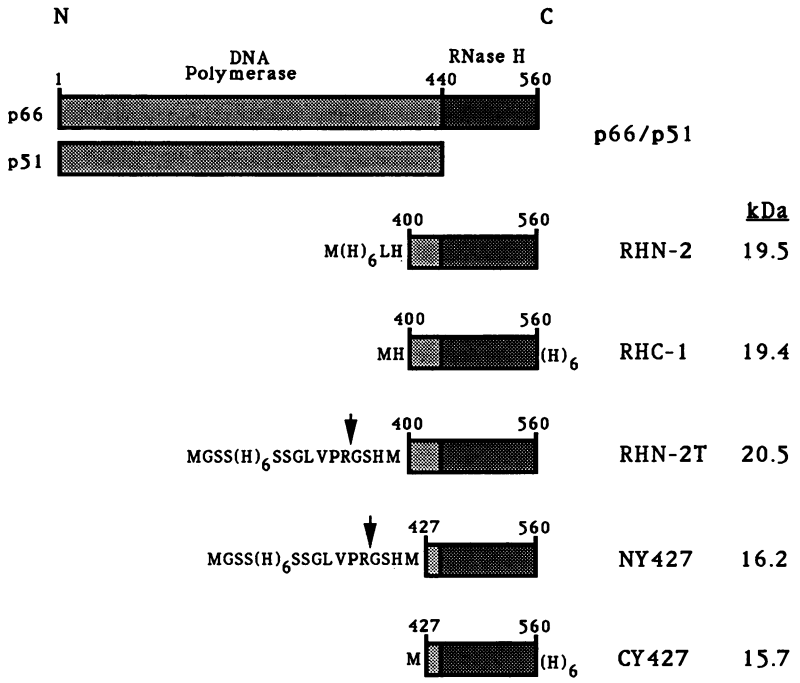

FIG. 1. Schematic representation of HIV-1 RNase H domain constructs. The DNA sequence encoding for either amino acids 400 to 560 or 427 to 560 of HIV-1 RT (HXB2) was cloned into the expression vector pET11c. An affinity tag consisting of six histidine residues was inserted at either the N or C terminus to facilitate purification by nickel-chelate affinity chromatography. The N-terminal extension derived from p51 consists of amino acids 400 to 440 or 427 to 440. RHN-2, RHN-2T, and NY427 are N-terminal-tagged constructs, while RHC-1 and CY427 are C-terminal-tagged constructs. RHN-2T and NY427 both have thrombin cleavage sites adjacent to the N-terminal histidine tag to facilitate removal of the tag following purification. The site of thrombin protease cleavage is indicated by an arrow. p66-p51 is the native HIV-1 RT. The calculated molecular masses for each protein are also indicated. Amino acid residues not derived from RT are represented as their single-letter symbols.

RHN2T is similar to pET-RHN2 except that it encodes a thrombin protease cleavage site between the N-terminal histidine tag and amino acid 400 of HIV-1 RNase H to facilitate removal of the six histidines after purification. Another PCR product encoding amino acids 427 to 510 was substituted for the N-terminal sequences in either pET-RHC1 or pET-RHN2T to produce the vector pET-CY427 or pET-NY427, respectively, which encodes for an RNase H domain consisting of amino acids 427 to 560 with a tag at either the C or N terminus. Figure 1 shows a schematic representation of the recombinant RNase H proteins produced by these expression vectors upon induction with IPTG. The predicted molecular masses for each of these recombinant proteins are also indicated in Fig. 1.

Recombinant RNase H proteins were extracted from *E. coli* with 4 M urea and chromatographed twice on Ni^{2+}-NTA columns. RHC-1 comprised approximately 5% of the total *E. coli* proteins (data not shown) and migrated as a 20-kDa protein (Fig. 2A, lane 1). The extracted protein was then loaded onto the first NTA column. The majority of nonspecific binding proteins were washed off at pH 6.3, while the majority of RHC-1 eluted at pH 4.5 (data not shown). These peak fractions were pooled and loaded onto a second NTA column (Fig. 2A, lane 1). Figure 2 shows the peak fractions of the second column purification step from a representative purification and Western blot of RHC-1 (panels A and B), as well as the pET11c vector control (panel C). RHN-2, RHN-2T, NY427, and CY427 all showed purification patterns similar to that of RHC-1 (data not shown). RHC-1 was not detected in the flowthrough, pH 8.0, or pH 6.3 step (lanes 2 to 5) by Coomassie staining. A small amount eluted in the pH 5.9 step (lanes 6 and 7), while the majority of RHC-1 eluted in four (1 ml) fractions in the pH 4.5 step (lanes 8 to 11). We estimate the pH 4.5 fractions to be approximately 90% pure. Each pH 4.5 fraction was renatured by slow dialysis and stored in 50% glycerol.

To confirm that the 20-kDa protein which eluted in the pH 5.9 and 4.5 steps was in fact an HIV-1-specific RNase H, a Western blot was performed on peak fractions from the RHC-1 purification (Fig. 2B). MAb 15 (43), which is specific for the C terminus of HIV-1 RNase H, recognized an approximately 20-kDa protein in only the pH 5.9 and 4.5 fractions, as expected. The minor contaminating proteins in the peak fractions visible by Coomassie staining are not HIV-1 RNase H derived, indicating that RHC-1 is a stable protein.

In Fig. 2C, a parallel purification of the pET11c vector induced in *E. coli* HMS174DE3 cells is shown. No 20-kDa proteins were detectable. However, the two contaminating proteins from the RHC-1 pH 4.5 24- and 13-kDa fractions were also detected in the control purification. The larger protein may be superoxide dismutase, which has been shown to bind the NTA resin (39a).

In Fig. 3A, the peak fraction of each of the purified proteins is shown after refolding. NY427 was also purified under native conditions as described in Materials and Methods. The refolded NY427 protein migrates identically to the native NY427 (compare lanes 5 and 6), indicating there was no detectable proteolysis during the native purification procedure.

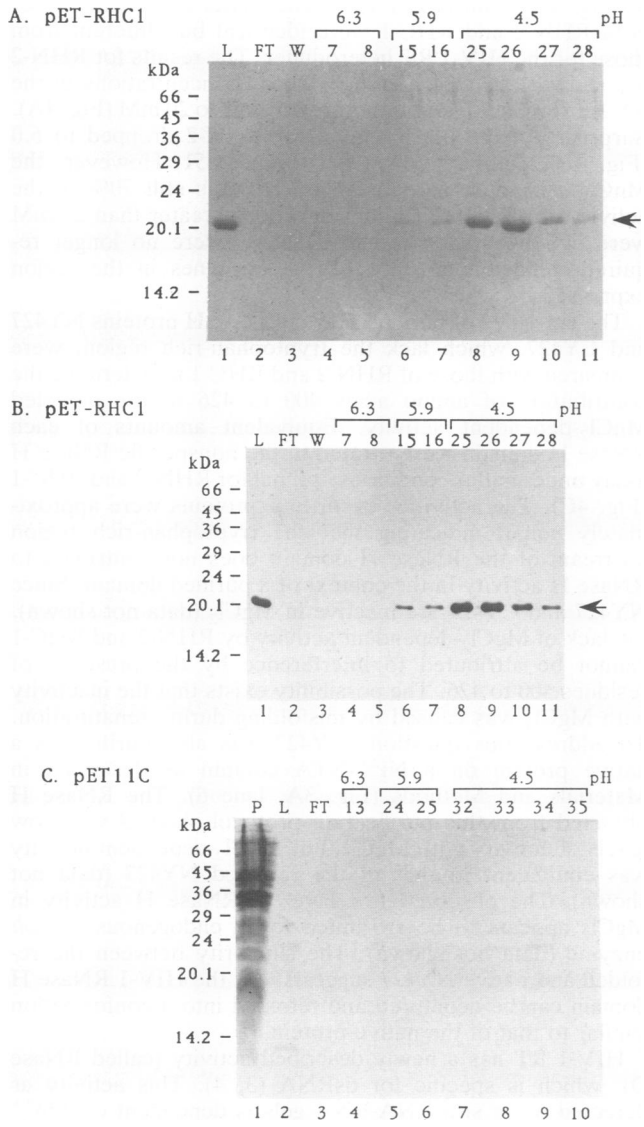

FIG. 2. Purification of HIV-1 RNase H on Ni^{2+}-nitrilotriacetate resin. *E. coli* containing either pET11c (expression vector without insert) or pET-RHC1 (C-terminal-tagged RNase H) was induced with IPTG and extracted with 4 M urea. The extracted material was passed through the NTA-agarose column and purified. The pH 4.5 peak fractions of the first column purification were pooled and passed through the column a second time. (A) Coomassie-stained SDS–17.5% polyacrylamide gel of the peak fractions from the second elution of the pET-RHC1 column. Lanes: 1, aliquot of the pooled pH 4.5 fractions loaded onto the second column (L); 2, protein which flowed through the column (FT); 3, protein which washed off at pH 8.0 (W); 4 to 11, peak protein fractions of each pH elution step (indicated above the lanes). (B) Western blot analysis of the peak pET-RHC1 fractions shown in panel A. Lanes: 1 to 3, load, flowthrough, and pH 8.0 wash, respectively; 4 to 11, peak fractions of each different pH elution step (indicated above the lanes). (C) Coomassie-stained SDS–17.5% polyacrylamide gel of the peak fractions from the second elution of the pET11c parent vector control. Lanes: 1 to 3, pellet, load, and flowthrough, respectively; 4 to 10, peak protein fractions of each different pH step (indicated above the lanes). The positions of molecular mass markers are on the left. The position of RHC-1 is identified by an arrow.

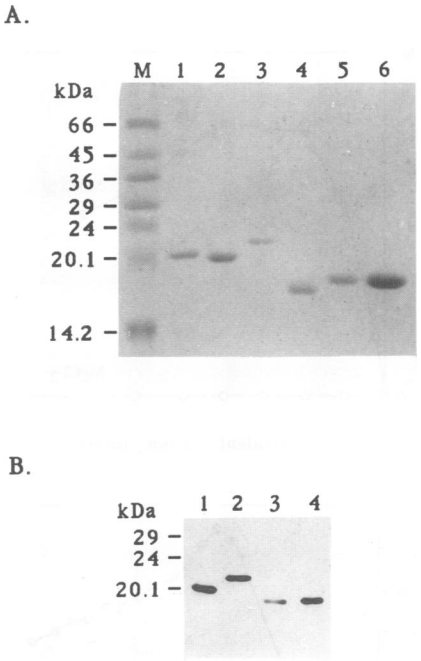

FIG. 3. (A) SDS-PAGE analysis of purified HIV-1 RNase H domains. The peak fraction of each of the purified proteins is shown on a Coomassie-stained 17.5% polyacrylamide gel following refolding of the denatured protein. Lanes: 1, RHN-2; 2, RHC-1; 3, RHN-2T; 4, CY427; 5, NY427; 6, NY427 after purification under native conditions; M, molecular size markers. (B) Removal of the N-terminal histidine tag. Purified RHN-2T was incubated with thrombin for 1.5 h at 25°C. Uncleaved material was bound to NTA resin. Cleavage was analyzed by Western blot with MAb 15. Lanes: 1, RHN-2; 2, RHN-2T; 3, RHN-2T following cleavage with thrombin; 4, thrombin-cleaved RHN-2T (material which did not bind to NTA resin). The sizes of molecular mass markers are shown on the left.

RHN-2T is similar to RHN-2 except it contains a thrombin cleavage site and flanking residues between the N-terminal histidine tag and the N-terminal RNase H residue Leu-400 to facilitate removal of the tag following purification (Fig. 1). The removal of the N-terminal histidine tag from purified RHN-2T is shown in Fig. 3B. Thrombin cleavage produced a truncated protein that, as expected, would no longer bind to the NTA resin (Fig. 3B, lane 4).

RHN-2 and RHC-1 have RNase H activity. The RNase H activity of the renatured His-tagged RNase H proteins was initially assayed by incubation with a circular RNA-DNA hybrid substrate labeled with [^{3}H]UTP under buffer conditions previously found to be optimal for HIV-1 RT RNase H activity (50). This RNase H assay is nonspecific. RHN-2 showed no detectable activity in the presence of $MgCl_2$ (Fig. 4A). Unexpectedly, the renatured RHN-2 fractions had high levels of RNase H activity in the presence of $MnCl_2$ (Fig. 4A). RHC-1 showed the same properties (data not shown). Negligible levels of activity were found in the control pET11c fractions with both $MnCl_2$ and $MgCl_2$, suggesting that any contaminating protein bands common to both the RNase H and control purifications were not RNase H enzymes.

Conditions for optimal RNase H activity were determined for both RHN-2 and RHC-1 and compared with those for wild-type HIV-1 RT. The optimal RNase H conditions for

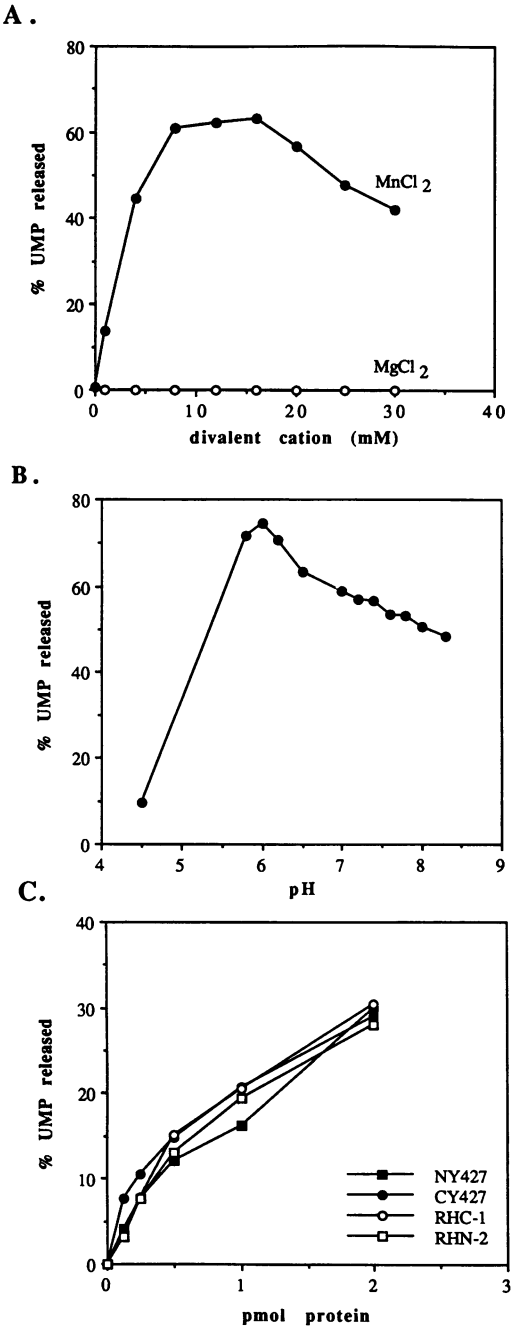

FIG. 4. Optimal reaction conditions for recombinant HIV-1 RNase H. The amounts of $MnCl_2$ and $MgCl_2$ (A) and the pH levels (B) were varied in the RNase H reaction to determine the optimal buffer conditions for RHN-2. In the $MnCl_2$ and $MgCl_2$ titrations, the other buffer component was 20 mM Tris-HCl (pH 8.0). The pH titration reactions contained 8 mM $MnCl_2$. For pH values 4.5 to 6.2, the buffer was 20 mM 2-(*N*-morpholino)ethanesulfonic acid (MES). For pH values 6.5 to 7.6, the buffer was 20 mM *N*-2-hydroxyethylpiperazine-*N'*-2-ethanesulfonic acid (HEPES), while for pH values 7.6 to 8.3, the buffer was 20 mM Tris-HCl. RHN-2 (4 pmol) was assayed for RNase H activity at 37°C for 30 min followed by TCA precipitation. (C) Comparison of the nonspecific RNase H activities of RHN-2 and RHC-1 to those of NY427 and CY427. Equivalent molar amounts of each purified RNase H domain were incubated with the substrate for 30 min at 37°C in optimal RHN-2 buffer (20 mM MES [pH 6.0], 8 mM $MnCl_2$) and then subjected to trichloroacetic acid precipitation.

HIV-1 RT are 50 mM Tris-HCl (pH 8.0), 50 mM KCl, 8 mM $MgCl_2$, and 2 mM DTT (50). The buffer requirements for both RHN-2 and RHC-1 were identical but different from those for the HIV-1 RT heterodimer. The results for RHN-2 are shown in Fig. 4. Optimal $MnCl_2$ concentrations in the RNase H reaction mixture ranged from 8 to 20 mM (Fig. 4A). Surprisingly, the pH optimum for RHN-2 dropped to 6.0 (Fig. 4B), compared with 8.0 for p66-p51. However, the $MnCl_2$-dependent activity at pH 8.0 was still 70% of the activity at pH 6.0. KCl concentrations greater than 25 mM were inhibitory, and reducing agents were no longer required, reflecting the absence of cysteines in the region expressed.

The activities of purified HIV-1 RNase H proteins NY427 and CY427, which lack the tryptophan-rich region, were compared with those of RHN-2 and RHC-1 to determine the contribution of amino acids 400 to 426 to the detected $MnCl_2$-dependent activity. Equivalent amounts of each RNase H domain were titrated in the nonspecific RNase H assay under buffer conditions optimal for RHN-2 and RHC-1 (Fig. 4C). The activities of all four proteins were approximately equal, indicating that the tryptophan-rich region upstream of the RNase H domain does not contribute to RNase H activity in the context of a purified domain. Since NY427 and CY427 are inactive in $MgCl_2$ (data not shown), the lack of $MgCl_2$-dependent activity by RHN-2 and RHC-1 cannot be attributed to interference by the presence of residues 400 to 426. The possibility exists that the inactivity with $MgCl_2$ was caused by misfolding during renaturation. To address this question, NY427 was also purified as a native protein on a Ni^{2+}-NTA column as described in Materials and Methods (Fig. 3A, lane 6). The RNase H obtained from this purification protocol showed very low levels of activity with $MgCl_2$, but $MnCl_2$-dependent activity was equivalent to that of the refolded NY427 (data not shown). The observed low level of RNase H activity in $MgCl_2$ appears to be attributed to an endogenous *E. coli* enzyme (data not shown). The similarity between the refolded and native NY427 suggests that the HIV-1 RNase H domain can be denatured and refolded into a conformation similar to that of the native protein.

HIV-1 RT has a newly described activity (called RNase D), which is specific for dsRNA (3, 4). This activity as detected on in situ RNA-RNA gels is dependent on Mn^{2+} (4). To determine whether the Mn^{2+}-dependent RNase H activity detected (Fig. 4) could actually be that of RNase D or of contaminating *E. coli* RNase III acting on fortuitous regions of dsRNA in the RNA-DNA hybrid substrate, we synthesized a dsRNA substrate and tested RHN-2 and RHC-1 for RNase D activity (Table 1). RHN-2 and RHC-1 did not have RNase D activity, while purified RNase III and the HIV-1 RT heterodimer were active, indicating that RHN-2 and RHC-1 do not have RNase D activity and that the preparations are not contaminated with RNase III. Further, *E. coli* RNase III was not detected in the purified RHN-2 or RHC-1 fractions by Western blot with a polyclonal antiserum specific for RNase III (data not shown).

There was also a possibility that the activity results shown in Fig. 4 were from a contaminating single-stranded RNase. To rule out this possibility, both the dsRNA and RNA-DNA hybrid substrates were heat denatured prior to incubation with RHN-2 and RHC-1 (Table 1). This procedure greatly diminished RNase H and dsRNA-dependent RNase activities; but in contrast, RNase A now completely degraded the RNA in both denatured substrates, indicative of the strand separation. The low levels of RNase III and RNase H

TABLE 1. Analysis of substrate integrity[a]

Protein or enzyme	RNA-RNA		RNA-DNA	
	Native	Denatured	Native	Denatured
RHN-2	−	−	++	±
RHC-1	−	−	++	±
HIV-1 RT	+	−	++	±
E. coli RNase H	−	−	++	±
RNase III	++	±	++	±
RNase A	±	++	+	++

[a] Substrates were incubated for 30 min at 37°C with saturating amounts of enzyme. The reactions were performed with the indicated amount of protein or enzyme activity level under the following conditions: for 5 pmol of RHN-2 or RHC-1, 20 mM MES (pH 6) or 20 mM Tris-HCl (pH 8), 8 mM $MnCl_2$, and 2 mM DTT; for 2 pmol of HIV-1 RT or 28 ng of RNase III, 20 mM Tris-HCl (pH 8), 8 mM $MnCl_2$, and 2 mM DTT; for 0.02 U of *E. coli* RNase H activity or 1 μg of RNase A, 20 mM Tris-HCl (pH 8), 8 mM $MgCl_2$, and 2 mM DTT. The results are expressed as the percentage of maximal substrate digestion levels as follows: ++, >75%; +, 31 to 75%; ±, 10 to 30%; and −, <10%.

activities detected following substrate denaturation are most likely due to a partial reannealing of the substrates at 37°C during the assays. These results indicate that the activity detected in the RHN-2 and RHC-1 preparations is truly an RNase H activity.

Purified *E. coli* RNase III was unexpectedly able to digest the [^{3}H]UTP-labeled RNA-DNA hybrid substrate under low salt concentrations (<100 mM) and in the presence of Mn^{2+} (Table 1). In low salt concentrations, RNase III has been previously shown to change structure and have reduced specificity or "star" activity which could explain this finding (10, 31). On the basis of the specificities of all the enzymes on each substrate, the data in Table 1 collectively indicate that the RNA-DNA hybrid is in fact a hybrid and that RNase III can digest this RNA-DNA hybrid. Further investigation of this property of *E. coli* RNase III is required.

In situ RNase H gel assays were performed to unambiguously attribute the activity detected in the RHN-2 and RHC-1 preparations to the recombinant HIV-1 proteins and not *E. coli* RNase H or other cellular proteins (Fig. 5). In situ assays have been applied for the rapid analysis of recombinant RT RNase H activity in a crude *E. coli* extract (53). For RHN-2 and RHC-1, the crude extract could not be analyzed, because *E. coli* RNase H (M_r, 18,000) would block out the HIV-1 signals. The purified proteins were fractionated on SDS-polyacrylamide gels which were copolymerized with a ^{32}P-labeled RNA-DNA hybrid substrate. The proteins within the gels were renatured; labeled RNA released from the hybrid by RNase H can diffuse from the gel, leaving a nonradioactive band on an autoradiograph that corresponds with the protein band after Coomassie staining. When the in situ gel was renatured in buffer containing $MnCl_2$ (Fig. 5A), both RHN-2 (lane 10) and RHC-1 (lane 12) showed RNase H activity, corresponding to the protein bands in lanes 4 and 6, respectively. The pET11c vector control fraction did not show any detectable activity (lanes 5 and 11). Importantly, there were no other zones of clearing detectable. Contaminating RNase H activities from the *E. coli* extract loaded on the column (lanes 1 and 7) were not present in the purified fractions. *E. coli* RNase III, shown to be active in this assay (lanes 3 and 9), was also not detected in the purified RNase H fractions. More RNase H activity was detected for RHC-1 than for RHN-2. RHC-1 may have refolded within the gel more efficiently than RHN-2 as a result of the histidine tag being at the C terminus. Even though more RHC-1 protein (4.4 μg) was loaded onto the gel than RHN-2 protein (4.0 μg), it is unlikely that this difference can account for the observed variation in activity. RNase H activity was not detected from RHN-2 or RHC-1 when the gel was soaked in buffer containing $MgCl_2$ (Fig. 5B), confirming the results of in-solution assay. The second band of clearing under the p66 band in both the Mn^{2+} and Mg^{2+} gels is most likely an N-terminal breakdown product of p66, since as expected, p51 (provided by Stuart Le Grice [29]) did not produce a signal (Fig. 5B, lanes 7 and 14). *E. coli* RNase III produced a band on the $MnCl_2$ gel (Fig. 5A, lane 9), as expected from the in-solution data in Table 1. In the presence of $MgCl_2$, RNase III does not digest the RNA-DNA hybrid in solution (data not shown). Therefore, the lack of clearing for RNase III in the $MgCl_2$ gel (Fig. 5B, lane 10) is not surprising. RNase III can digest dsRNA in the presence of $MgCl_2$. Since $MgCl_2$-dependent activity is not detected with RNase III on the RNA-DNA hybrid substrate, this indicates that there is minimal dsRNA in the hybrid preparation.

RNase H activity relative to intact HIV-1 RT. A time course of RNase H activity for RHN-2, RHC-1, HIV-1 RT, and the pET11c control was determined with the nonspecific ^{3}H-labeled substrate under optimal buffer conditions for each of the proteins (Fig. 6). The accumulation of acid-soluble radioactivity in the supernatant was monitored over a course of 10 min. RHN-2 and RHC-1 showed almost identical kinetics on this substrate, suggesting that the orientation of the histidine tag does not play a major role in RNase H activity. On a molar basis, the wild-type HIV-1 RT heterodimer was approximately threefold more active than either RHN-2 or RHC-1 when Mn^{2+} was the divalent cation in the reaction. RHN-2 had a specific activity of 650 U/mg and RHC-1 had a specific activity of 750 U/mg, while that of the HIV-1 RT heterodimer was 350 U/mg. An RNase H unit of activity is defined as 1 pmol of [^{3}H]UMP released in 1 min.

The effects of several inhibitors of HIV-1 RNase H activity are given in Table 2. dAMP (20 mM), previously determined to inhibit the RNase H activity of HIV-1 RT (52), was a better inhibitor of RHC-1 and RHN-2 than of HIV-1 RT. RVC (8 mM) completely eliminated activity from all three proteins, while RNasin did not inhibit any protein, as expected from previous studies (26). Interestingly, MAb 18D7, previously found to inhibit the RNase H activity of HIV-1 RT (51), almost completely inhibited RHN-2 and RHC-1 activities. The epitope recognized by this MAb has been mapped to the RNase H domain. Another MAb (7E5), which recognizes a conformational epitope of the RNase H domain but does not inhibit RNase H activity in the case of heterodimeric RT (51), did inhibit RHN-2 and RHC-1 by approximately 95% (data not shown). MAb 20 (43), which does not recognize the HIV-1 RNase H domain, did not inhibit the RNase H activity (data not shown). These results suggest the RNase H activity of the isolated RNase H domain with an N-terminal extension back to threonine 400 retains many characteristics of the wild-type enzyme. Also, in the absence of the entire p66-p51, the RNase H domain is more susceptible to inhibitors than as a heterodimer.

Specificity of minus-strand primer removal by recombinant HIV-1 RNase H domain. Previous studies have demonstrated that the RNase H activity of HIV-1 RT specifically removes the $tRNA_3^{Lys}$ minus-strand primer in vitro, cleaving one nucleotide away from the U5-primer binding site junction (12, 39, 48). This specific cleavage results in the 3′ rA of the $tRNA_3^{Lys}$ being left attached to the U5 long terminal repeat terminus. In Fig. 7, RHN-2T was tested for the ability to produce the same specific cleavage event as the wild-type heterodimer by using a model substrate. This substrate

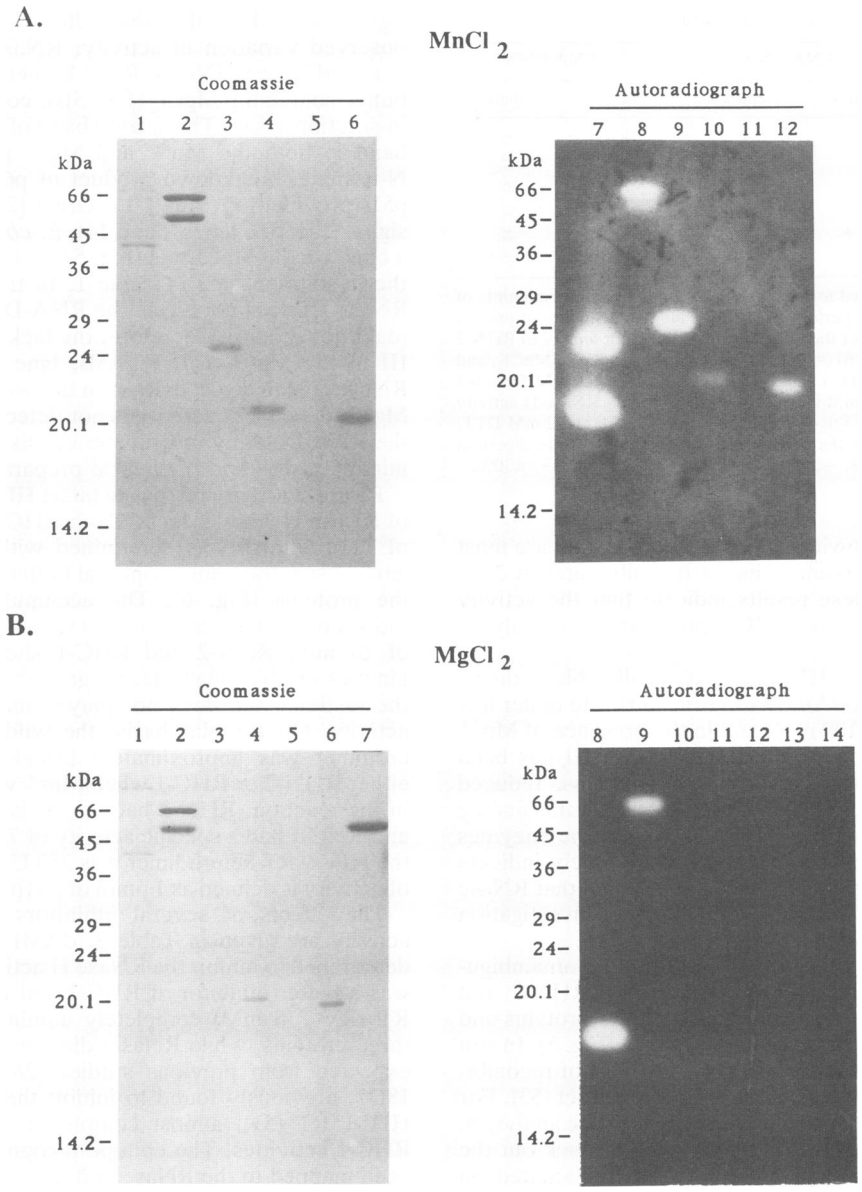

FIG. 5. In situ RNase H gel assay. Approximately 6×10^6 cpm of a [^{32}P]CTP-labeled RNA-DNA hybrid was copolymerized into an SDS–17.5% polyacrylamide gel. Following electrophoresis of the purified RHN-2 and RHC-1 proteins, the gel was soaked in a renaturation buffer (50 mM Tris-HCl [pH 8.0], 50 mM KCl, 8 mM $MgCl_2$ or $MnCl_2$ as indicated, 2 mM DTT) at room temperature for at least 3 days. The gel was exposed wet for autoradiography and then stained with Coomassie brilliant blue. (A) Coomassie stain and activity gel with 8 mM $MnCl_2$. Lanes: 1 and 7, *E. coli* 4 M urea extract loaded onto the first pET-RHC1 NTA column; 2 and 8, purified HIV-1 RT heterodimer (5.2 μg); 3 and 9, purified *E. coli* RNase III (0.7 μg); 4 and 10, purified RHN-2 (4 μg); 5 and 11, pET11c control; 6 and 12, purified RHC-1 (4.4 μg). (B) Coomassie stain and activity gel with 8 mM $MgCl_2$. Amounts of protein identical to those for the $MnCl_2$ gel were loaded. Lanes: 1 and 8, *E. coli* 4 M urea extract of the pET-RHC1 purification; 2 and 9, HIV-1 RT; 3 and 10, *E. coli* RNase III; 4 and 11, RHN-2; 5 and 12, pET11c control; 6 and 13, RHC-1; 7 and 14, purified p51 polymerase domain (4 μg) of HIV-1 RT. The positions of molecular mass markers (in kilodaltons) are shown to the left of each gel.

mimics an intermediate in reverse transcription where plus-strand synthesis has been completed after the first 18 nucleotides of the tRNA minus-strand primer have been copied (48). Upon incubation with RHN-2T, the major product produced migrates as a species 108 nucleotides long, corresponding to the size expected for the correct specific cleavage (Fig. 7, lanes 1 to 4). Interestingly, removal of the histidine tag by cleavage with thrombin, as seen in Fig. 3B, abolishes RNase H activity (Fig. 7, lanes 5 to 8). However, the specific cleavage can be recovered by the addition of the purified HIV-1 RT p51 subunit (lanes 9 to 12). The addition of p51 does not completely restore the original activity level, as shown by the time course data (compare lanes 1 to 4 with 9 to 12). Activity is not detected when p51 is incubated without RHN-2T (lanes 13 to 16). A similar cleavage pattern is also observed when the release of the RNA is assayed directly (data not shown) as has been demonstrated for the HIV-1 RT heterodimer (48). It might be expected that since

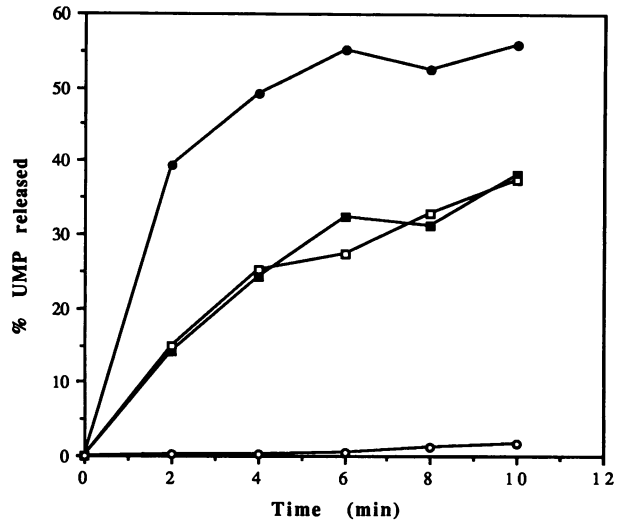

FIG. 6. Comparison of RNase H activities of the extended RNase H domain to that of wild-type HIV-1 RT under optimal reaction conditions for each RNase H. RNase H activity was monitored over a course of 10 min with aliquots taken every 2 min. Protein (1 pmol) was added to each reaction. For the pET11c control, an equivalent amount of fraction volume was added since the protein concentration was much lower than that for the N- and C-terminal-tagged RNase H domain fractions. Buffer conditions for wild-type HIV-1 RT (●) were 50 mM Tris-HCl (pH 8.0), 50 mM KCl, 8 mM $MnCl_2$, and 2 mM DTT. Buffer conditions for RHN-2 (■), RHC-1 (□), and the pET11c control fraction (○) were 20 mM MES (pH 6.0), 8 mM $MnCl_2$, and 2 mM DTT.

HIV-1 RNase H and *E. coli* RNase H are so similar structurally, they would produce a similar cleavage pattern. However, *E. coli* RNase H produced a random cleavage pattern (data not shown). These results indicate that the RNase H domain of RT is directly responsible for the specificity of $tRNA_3^{Lys}$ removal in vitro. The polymerase domain does not appear to contribute to the specific cleavage observed in this assay. Removal of the histidine tag from RHN-2T also abolished activity on the nonspecific RNase H substrate (data not shown). It appears that the histidine tag is providing a function usually provided by the p51 subunit.

Recombinant HIV-1 RNase H is a monomer. Previous studies have shown antibodies directed against the tether region can inhibit dimerization (43). Since a portion of the tether-connector subdomain has been included in the recombinant RHN-2 and RHC-1 RNase H proteins, there was a possibility that dimers could form. Zonal centrifugation was performed with the N-terminal-tagged RNase H protein (RHN-2) on a linear 10 to 30% glycerol gradient to determine the oligomerization state of the enzyme (Fig. 8). On the RHN-2 gradient, RNase H activity peaked at fraction 24, corresponding to the sedimentation expected for a protein with a molecular mass of approximately 20 to 21 kDa. The M_r of RHN-2 on an SDS-polyacrylamide gel is 20,000. Therefore, in this buffer system, RHN-2 behaves as a monomer. Fraction 24 contained the peak of the RHN-2 protein, detected by Western blot (data not shown), indicating that the protein and the enzyme comigrated. RHN-2 was not detected in the fractions corresponding to the sedimentation position expected for a dimer. These results suggest that the N-terminal p51-derived extension on RHN-2 (amino acids 400 to 440) is not sufficient for dimerization. RHC-1 with a C-terminal histidine tag also sedimented as a monomer (data not shown), suggesting that dimerization is not simply being blocked by the histidine tag.

TABLE 2. Effects of known HIV-1 RNase H inhibitors

Protein	% Inhibition by[a]:				
	RVC	dAMP	MAb 18D7	Acetonitrile	RNasin
RHN-2	100	84	98	8	1
RHC-1	100	80	98	4	0
p66-p51	100	42	80	100	5

[a] Data are the averages from at least two independent assays. One picomole of each protein was used in the RNase H reaction mixtures. Proteins and inhibitors were preincubated for 10 min on ice prior to the addition of the substrate. Reactions were stopped after 4 min. The concentration or amount of inhibitor used was 8 mM RVC, 20 mM dAMP, 2 μg of MAb 18D7, 15% acetonitrile, or 0.8 U of RNasin per μl.

DISCUSSION

Previous studies using model substrates in vitro have concluded that the RNase H activity of HIV-1 RT incompletely removes the $tRNA_3^{Lys}$ minus-strand primer (12, 39, 48). The cleavage specificity observed resulted in the 3′-rA nucleotide of the $tRNA_3^{Lys}$ CCA-3′ terminus remaining attached to the adjacent U5 DNA sequence. This specificity explains the presence of an extra A:T base pair detected in the majority of HIV-1 circle junction sequences (20, 28, 35, 47, 57). The mechanism directing this specificity remains unclear. The specificity can occur in both the presence and absence of DNA polymerization. However, in the absence of DNA polymerization, the specificity may be dependent on a sequence or structural feature of the tRNA-DNA junction region. Changing the rA to deoxyadenosine 5′ phosphate does not alter the specificity (48). After this paper had been submitted for publication, a paper describing unusual sugar conformations for the first two DNA residues of the $tRNA_3^{Lys}$ hybrid junction was published (45). Given the ability of HIV-1 RT to produce the specific cleavage in both the polymerase-dependent and -independent modes, and since the polymerase domain is believed to provide the substrate-binding cleft, we wanted to determine the actual contribution of the polymerase domain to the minus-strand primer removal specificity.

Previous studies have concluded that there is a large degree of interdependence between the DNA polymerase and RNase H domains of HIV-1 RT (5, 17, 38). Further, the RNase H and DNA polymerase active sites share a single substrate-binding cleft (1, 25). This cleft is formed primarily by the DNA polymerase domain consisting of the N-terminal 51-kDa portion of p66. There has been considerable controversy regarding whether the HIV-1 RNase H domain can function alone without the presence of the DNA polymerase domain. Several groups have expressed and purified HIV-1 RNase H domains which were inactive or had very low levels of activity (2, 8, 42, 49). These constructs generally consisted of amino acids 427 to 560 and therefore lacked the substrate-binding cleft. However, there have also been reports of active RNase H domains (11, 16), one of which was purified from virions and the other of which had a histidine tag at the N terminus. RNase H activity can be reconstituted between an inactive p15 domain and purified p51 (21), again suggesting that in the context of the p66 subunit, residues of the polymerase domain are important for RNase H activity. Possibly, amino acids immediately N-terminal of the RNase H domain, specifically regions of the connector subdomain

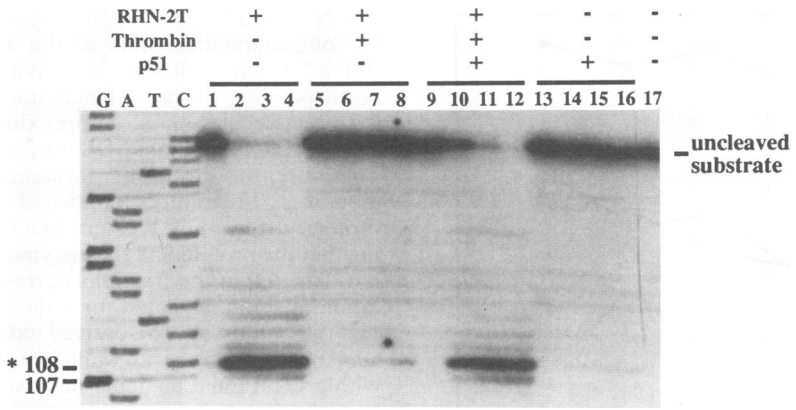

FIG. 7. Specificity of $tRNA_3^{Lys}$ primer removal by RHN-2T. The substrate for determining the site of cleavage in the minus-strand primer removal was incubated with the isolated RNase H domain RHN-2T for either 0, 5, 30, or 45 min at 37°C. RNase cleavage products were analyzed on a 10% sequencing gel. A sequencing ladder (lanes G, A, T, and C) consisting of single-stranded pMR2S-1 DNA primed with the 18-mer oligodeoxynucleotide 2641, which is complementary to PBS, was used as a marker. Lanes: 1 to 4, RHN-2T (100 ng) incubated with substrate for 0, 5, 30, and 45 min, respectively; 5 to 8, thrombin-cleaved RHN-2T (100 ng) incubated for 0, 5, 30, and 45 min, respectively; 9 to 12, thrombin-cleaved RHN-2T (100 ng) plus purified p51 subunit (50 ng) incubated with substrate for 0, 5, 30, and 45 min, respectively; 13 to 16, p51 incubated with substrate for 0, 5, 30, and 45 min, respectively; 17, substrate incubated alone for 45 min. The position of the uncleaved substrate is indicated on the right. The cleavage product expected for complete RNA removal at the RNA-DNA junction is 107 nucleotides, while position 108 corresponds to specific cleavage 5′ of the rA residue. This major cleavage product is also indicated by an asterisk.

that form the interface with RNase H, have a role in RNase H activity. There is a tryptophan-rich region upstream of Tyr-427 for which there is a counterpart in *E. coli* RNase H. There have been suggestions that this tryptophan-rich region could play a role in substrate binding (8).

To determine whether amino acids upstream from Tyr-427, specifically the tryptophan-rich region, contribute to RNase H activity in the context of an isolated domain, and to determine whether the HIV-1 RNase H domain can specifically remove the $tRNA_3^{Lys}$ minus-strand primer in the absence of the polymerase domain, we have expressed and purified from *E. coli* an HIV-1 RNase H domain consisting of amino acids 400 to 560 of RT. The protein was tagged at either the N or C terminus with six histidine residues, expressed in *E. coli*, purified under denaturing conditions by Ni^{2+}-NTA chelate chromatography, and characterized. Both renatured RNase H proteins, RHN-2 and RHC-1, had Mn^{2+}- but not Mg^{2+}-dependent RNase H activity. This activity was approximately threefold less on a molar basis than the intact p66-p51 heterodimer in $MnCl_2$. The lower activity may be due to decreased processivity (16). In situ RNase H assays of our purified HIV-1 RNase H proteins (Fig. 5) found no detectable *E. coli* RNase H. It has been suggested that the low level of activity detected with one of the other purified HIV RNase H domains is from a contaminating *E. coli* enzyme (42). The recombinant RNase H proteins, NY427 and CY427, which lack the tryptophan-rich region, had the same levels of Mn^{2+}-dependent activity as RHN-2 and RHC-1. This similarity ruled out the possibility that residues 400 to 426 were playing a role in RNase H activity in the context of these proteins. The low level of Mg^{2+}-dependent activity in the native NY427 preparation was attributed to a contaminating *E. coli* protein. This result is in contrast with the report of an (amino acids 427 to 560) HIV-1 RNase H with an alternate N-terminal tag that was found to be enzymatically active with Mg^{2+} as the divalent cation (11).

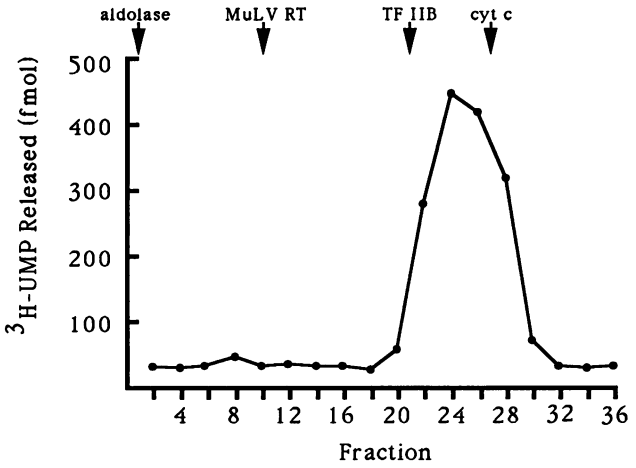

FIG. 8. Zonal centrifugation of purified RHN-2. RHN-2 (16 μg) was diluted into 250 μl and layered onto a 4.75-ml linear gradient of 10 to 30% glycerol in a buffer consisting of 50 mM Tris-HCl (pH 8.0), 50 mM KCl, 2 mM DTT, 0.1 mM EDTA, and 0.01% Triton X-100. The gradient was centrifuged at 48,000 rpm in a Sorvall AH-650 rotor for 24 h at 4°C. Fractions (125 μl) were collected from the bottom of the tube, and 5 μl of each fraction was assayed for RNase H activity as described in Materials and Methods. Cytochrome *c* (12.4 kDa), TFIIB (33 kDa), Mo-MuLV RT (71 kDa), and aldolase (160 kDa) were sedimented in a separate tube under identical conditions. All of these proteins sedimented as monomers, except for aldolase, which is a tetramer. The positions of the protein markers are indicated by arrows.

RNase H activity was optimal at pH 6 rather than the pH 8 optimum of the intact RT heterodimer. Since the pK_a of the imidazole group of histidine is 6, it seemed likely that the histidine tag was playing a role in the observed RNase H activity. One of the reported active amino acid 427 to 560 RNase H domains also had an affinity tag at the N terminus containing histidine residues (11). Removal of the N-terminal

histidine tag from RHN-2T by cleavage with thrombin resulted in an inactive protein. Interestingly, the protease site of NY427 was resistant to thrombin cleavage (data not shown), suggesting that the thrombin site is more tightly associated with the RNase H structure of NY427 than for RHN-2T. The presence of the tryptophan-rich region (amino acids 400 to 426) resulted in the RNase H being expressed as an insoluble protein. The role the tag is playing remains unclear.

Upon incubation of RHN-2T with the model substrate for $tRNA_3^{Lys}$ removal, the major cleavage product corresponded to the size expected for release of the RNA primer leaving the 3′-rA residue attached to U5 sequences (Fig. 7). Despite the requirement for the histidine tag, the isolated RNase H domain retained the same specificity for $tRNA_3^{Lys}$ removal as the wild-type heterodimer. The requirement for the histidine tag could be overcome by the addition of the purified p51 subdomain to the thrombin-cleaved RNase H, suggesting that the histidine tag is playing a role usually provided by p51, either substrate binding or stabilization. Since the cleavage specificity of an isolated RNase H domain was the same as that for the wild-type HIV-1 RT heterodimer, the polymerase domain probably does not play a direct role in controlling the specificity of $tRNA_3^{Lys}$ removal through recognition of sequence or structure by the substrate-binding cleft.

E. coli RNase H is structurally very similar to HIV-1 RNase H. One notable difference is the presence of a lysine-rich handle region consisting of a loop and α-helix C in *E. coli* RNase H, which is missing in the case of HIV (8, 24, 60). Substitutions of the lysines in this handle region raise the K_m while not affecting V_{max}, suggesting a role in substrate binding (23). Since at pH 6 the histidine tag would be more positively charged than at pH 8, it is possible that the histidine tag of RHN-2 and RHC-1 could be playing a role in substrate binding, substituting for the positively charged lysine-rich region of *E. coli* RNase H. Computer modeling of the histidine tags onto the RNase H structure indicated the N- and C-terminal tags localize to nonoverlapping regions of the protein. In either case, though, the histidine tag could potentially come in contact with nucleic acid, which could increase substrate binding.

Although it is unlikely that the histidine tags could be stabilizing identical regions of the protein, the possibility still exists that the histidine tag is stabilizing the RNase H structure. In the crystal structure of HIV-1 RNase H, amino acids 538 to 542 are disordered, including the highly conserved His-539 (8). Further, the entire C terminus of an HIV-1 RNase H domain in solution is disordered from amino acids 536 to 560 as determined by nuclear magnetic resonance (36). Mutations of the conserved His-539 residue have reduced exonuclease activity, are more sensitive to salt, and may show reduced substrate binding (46, 59). In *E. coli* RNase H, however, mutations of the conserved histidine-124 decrease the V_{max} without affecting the K_m, suggesting that the histidine is involved in catalysis rather than substrate binding (34). In the crystal structure of the HIV-1 RT heterodimer, this His-539 loop is ordered and interacts with a portion of the p51 thumb subdomain (25). The His-539 loop is also in close proximity to two divalent metal ions, again suggesting an involvement of this region in RNase H activity. Similarly, two Mn^{2+} ions are bound in the isolated RNase H domain structure (8). The disorder of the His-539 loop has been suggested to be the reason for inactivity of isolated RNase H domains consisting of residues 427 to 560 (8, 25, 37). For RHN-2 and RHC-1, the histidine tag could be playing a role in stabilizing the C terminus, either directly (C-terminal tag) or indirectly (N-terminal tag).

A recent study has demonstrated that a mutation of glutamic acid-478 eliminates both HIV-1 RNase H activity and the newly discovered dsRNA-dependent RNase activity (RNase D), suggesting that the two activities have either overlapping or identical catalytic sites (4). RHN-2 and RHC-1 did not have detectable RNase D activity but did have RNase H activity. Like RNase H, RNase D may be dependent on the DNA polymerase domain for activity. Mo-MuLV RT also contains the double-stranded RNase activity (4, 14). However, an isolated RNase H domain of Mo-MuLV RT does not have RNase D activity (14), in agreement with our results with the isolated HIV RNase H domain.

RHN-2 and RHC-1 were generally more sensitive to inhibitors of RNase H activity than was the HIV-1 RT heterodimer (Table 2). The structure of HIV-1 RT revealed that the thumb of the p51 subunit interacts with RNase H (25). The lack of this intersubunit contact as well as other interactions that normally occur with the polymerase domain of p66 most likely makes RHN-2 and RHC-1 more sensitive to inhibitors of HIV-1 RNase H activity, including dAMP, MAb 18D7, and RVC. RVC is believed to inhibit the RNase H activity of HIV-1 RT by binding to the substrate-binding cleft (27). The finding that RHN-2 and RHC-1 are inhibited by RVC indicates that there is another mode of action for the RVC inhibition of RNase H.

Epitope mapping studies and the crystal structure of the HIV-1 RT heterodimer implicate the tether-connection subdomain as being important for dimerization between p51 and p66 (25, 43). In addition, it has been shown that this dimerization is required for the RNase H activity of HIV-1 RT (42). RHN-2 and RHC-1, however, behaved as monomers on a glycerol gradient, suggesting that under the conditions tested, amino acids 400 to 440 are not sufficient for dimerization, even though most of the tryptophan-rich region is present. In addition, 15% acetonitrile (Table 2), which has been used to dissociate the HIV-1 heterodimer (41, 42), had very little effect on the RNase H activity of RHN-2 or RHC-1, while greatly affecting the heterodimer. The RNase H domain described by Becerra et al. behaved as a monomer and had very low activity (2). However, the RNase H domain described by Restle et al. fractionated as an inactive monomer and putative dimer (42). While the data of Restle et al. (42) indicate that in the context of full-length RT, dimerization is required for RNase H activity, monomeric RHN-2 and RHC-1 are active. In the context of an isolated domain, the unusual requirement of a histidine tag for activity may somehow be substituting for contacts usually made between the p66 and p51 subunits.

In the process of studying the specificity of $tRNA_3^{Lys}$ minus-strand primer removal, we have characterized the activity of an isolated HIV-1 RNase H domain. Residues 400 to 426, which encompass the tryptophan-rich region of the connector subdomain, did not contribute to the Mn^{2+}-dependent RNase H activity of this protein. In addition, activity was dependent on a histidine affinity tag being present at either the N or C terminus. Despite the requirement for a histidine tag, the isolated RNase H enzymes retained many characteristics of RNase H in the context of a heterodimer, including the specific removal of $tRNA_3^{Lys}$.

ACKNOWLEDGMENTS

We thank Jeffrey Culp for the gift of recombinant HIV-1 RT. We also thank Vinayaka Prasad for the gift of monoclonal antibodies

18D7 and 7E5, Tobias Restle for monoclonal antibodies 15 and 20, Stuart Le Grice for purified HIV-1 RT p51 subunit, Bradley Preston for the plasmid pRT4, Paul March for purified *E. coli* RNase III and polyclonal RNase III antiserum, and Danny Reinberg for purified TFIIB and TFIIB polyclonal antiserum. We thank Paul March and Alfredo Jacobo-Molina for discussion of the manuscript.

This work was supported by grant R01-CA49932 from the National Institutes of Health. M.J.R. is a recipient of the Leukemia Society of America, Inc., Scholar Award. J.S.S. is a recipient of the New Jersey Commission on Cancer Research Predoctoral Fellowship no. 691-037-F2.

REFERENCES

1. **Arnold, E., A. Jacobo-Molina, R. G. Nanni, R. L. Williams, X. Lu, J. Ding, J. Arthur, D. Clark, A. Zhang, A. L. Ferris, P. Clark, A. Hizi, and S. H. Hughes.** 1992. Structure of HIV-1 reverse transcriptase/DNA complex at 7A resolution showing active site locations. Nature (London) **357:**85–89.
2. **Becerra, S. P., G. M. Clore, A. M. Gronenborn, A. R. Karlstrom, S. J. Stahl, S. H. Wilson, and P. T. Wingfield.** 1990. Purification and characterization of the RNase H domain of HIV-1 reverse transcriptase expressed in recombinant *Escherichia coli*. FEBS Lett. **270:**76–80.
3. **Ben-Artzi, H., E. Zeelon, M. Gorecki, and A. Panet.** 1992. Double-stranded RNA-dependent RNase activity associated with human immunodeficiency virus type 1 reverse transcriptase. Proc. Natl. Acad. Sci. USA **89:**927–931.
4. **Ben-Artzi, H., E. Zeelon, S. F. J. Le-Grice, M. Gorecki, and A. Panet.** 1992. Characterization of the double stranded RNA dependent RNase activity associated with recombinant reverse transcriptases. Nucleic Acids Res. **20:**5115–5118.
5. **Boyer, P. L., A. L. Ferris, and S. H. Hughes.** 1992. Cassette mutagenesis of the reverse transcriptase of human immunodeficiency virus type 1. J. Virol. **66:**1031–1039.
6. **Bradford, M. M.** 1976. A rapid and sensitive method for the quantitation of microgram quantities of protein utilizing the principle of protein-dye binding. Anal. Biochem. **72:**248–254.
7. **Coffin, J. M.** 1990. Retroviridae and their replication, p. 1437–1500. *In* B. N. Fields, D. M. Knipe, R. M. Chanock, M. S. Hirsch, J. L. Melnick, T. P. Monath, and B. Roizman (ed.), Virology, 2nd ed. Raven Press, Ltd., New York.
8. **Davies, J. F., III, Z. Hostomska, Z. Hostomsky, S. R. Jordan, and D. A. Matthews.** 1991. Crystal structure of the ribonuclease H domain of HIV-1 reverse transcriptase. Science **252:**88–95.
9. **DiMarzo Veronese, F., T. D. Copeland, A. L. DeVico, R. Rahman, S. Oroszlan, R. C. Gallo, and M. G. Sarngadharan.** 1986. Characterization of highly immunogenic p66/p51 as the reverse transcriptase of HTLV-III/LAV. Science **231:**1289–1291.
10. **Dunn, J. J.** 1976. RNase III cleavage of single-stranded RNA. Effect of ionic strength on the fidelity of cleavage. J. Mol. Biol. **251:**3807–3814.
11. **Evans, D. B., K. Brawn, J. Martin, R. Deibel, W. G. Tarpley, and S. K. Sharma.** 1991. A recombinant ribonuclease H domain of HIV-1 reverse transcriptase that is enzymatically active. J. Biol. Chem. **266:**20583–20585.
12. **Furfine, E. S., and J. E. Reardon.** 1991. Human immunodeficiency virus reverse transcriptase ribonuclease H: specificity of $tRNA^{Lys3}$-primer excision. Biochemistry **30:**7041–7046.
13. **Furfine, E. S., and J. E. Reardon.** 1991. Reverse transcriptase-RNase H from the human immunodeficiency virus. J. Biol. Chem. **266:**406–412.
14. **Goff, S. (Columbia University).** 1993. Personal communication.
15. **Gopalakrishnan, V., J. A. Peliska, and S. J. Benkovic.** 1992. Human immunodeficiency virus type 1 reverse transcriptase: spatial and temporal relationship between the polymerase and RNase H activities. Proc. Natl. Acad. Sci. USA **89:**10763–10767.
16. **Hansen, J., T. Schulze, W. Mellert, and K. Moelling.** 1988. Identification and characterization of HIV-specific RNase H by monoclonal antibody. EMBO J. **7:**239–243.
17. **Hizi, A., S. H. Hughes, and M. Shaharabany.** 1990. Mutational analysis of the ribonuclease H activity of human immunodeficiency virus 1 reverse transcriptase. Virology **175:**575–580.
18. **Hochuli, E., W. Bannwarth, H. Dobeli, R. Gentz, and D. Stuber.** 1988. Genetic approach to facilitate purification of recombinant proteins with a novel metal chelate adsorbent. Bio/Technology **6:**1321–1325.
19. **Hoffmann, A., and R. G. Roeder.** 1991. Purification of his-tagged proteins in non-denaturing conditions suggests a convenient method for protein interaction studies. Nucleic Acids Res. **19:**6337–6338.
20. **Hong, T., K. Drlica, A. Pinter, and E. Murphy.** 1991. Circular DNA of human immunodeficiency virus: analysis of circle junction nucleotide sequences. J. Virol. **65:**551–555.
21. **Hostomsky, Z., Z. Hostomska, G. O. Hudson, E. W. Moomaw, and B. R. Nodes.** 1991. Reconstitution *in vitro* of RNase H activity by using purified N-terminal and C-terminal domains of human immunodeficiency virus type 1 reverse transcriptase. Proc. Natl. Acad. Sci. USA **88:**1148–1152.
22. **Jonsson, C. B., G. A. Donzella, and M. J. Roth.** 1993. Characterization of the forward and reverse reactions of the Moloney murine leukemia virus integrase protein purified from *Escherichia coli*. J. Biol. Chem. **268:**1462–1469.
23. **Kanaya, S., C. Katsuda-Nakai, and M. Ikehara.** 1991. Importance of the positive charge cluster in *Escherichia coli* ribonuclease HI for the effective binding of the substrate. J. Biol. Chem. **266:**11621–11627.
24. **Katayanagi, K., M. Miyagawa, M. Matsushima, M. Ishikawa, S. Kanaya, M. Ikehara, T. Matsuzaki, and K. Morikawa.** 1990. Three-dimensional structure of ribonuclease H from *E. coli*. Nature (London) **347:**306–309.
25. **Kohlstaedt, L. A., J. Wang, J. M. Friedman, P. A. Rice, and T. A. Steitz.** 1992. Crystal structure at 3.5 Å resolution of HIV-1 reverse transcriptase complexed with an inhibitor. Science **256:**1783–1790.
26. **Krug, M. S., and S. L. Berger.** 1989. Ribonuclease H activities associated with viral reverse transcriptases are endonucleases. Proc. Natl. Acad. Sci. USA **86:**3539–3543.
27. **Krug, M. S., and S. L. Berger.** 1991. Reverse transcriptase from human immunodeficiency virus: a single template-primer binding site serves two physically separable catalytic functions. Biochemistry **30:**10614–10623.
28. **Kulkosky, J., R. A. Katz, and A. M. Skalka.** 1990. Terminal nucleotides of the preintegrative linear form of HIV-1 DNA deduced from the sequence of circular DNA junctions. J. Acquired Immune Defic. Syndr. **3:**852–858.
29. **Le Grice, S. F. J., T. Naas, B. Wohlensinger, and O. Schatz.** 1991. Subunit-selective mutagenesis indicates minimal polymerase activity in heterodimer-associated p51 HIV-1 reverse transcriptase. EMBO J. **10:**3905–3911.
30. **Lightfoote, M. M., J. E. Coligan, T. M. Folks, A. S. Fauci, M. A. Martin, and S. Venkatesan.** 1986. Structural characterization of reverse transcriptase and endonuclease polypeptides of the acquired immunodeficiency syndrome retrovirus. J. Virol. **60:**771–775.
31. **March, P. E., and M. A. Gonzalez.** 1990. Characterization of the biochemical properties of recombinant ribonuclease III. Nucleic Acids Res. **18:**3293–3298.
32. **Mizrahi, V., G. M. Lazarus, L. M. Miles, C. A. Meyers, and C. DeBouck.** 1989. Recombinant HIV-1 reverse transcriptase: purification, primary structure, and polymerase/ribonuclease H activities. Arch. Biochem. Biophys. **273:**347–358.
33. **Mous, J., E. P. Heimer, and S. F. J. Le Grice.** 1988. Processing protease and reverse transcriptase from human immunodeficiency virus type 1 polyprotein in *Escherichia coli*. J. Virol. **62:**1433–1436.
34. **Oda, Y., M. Yoshida, and S. Kanaya.** 1993. Role of histidine 124 in the catalytic function of ribonuclease HI from *Escherichia coli*. J. Biol. Chem. **268:**88–92.
35. **Pauza, C. D.** 1990. Two bases are deleted from the termini of HIV-1 linear DNA during integrative recombination. Virology **179:**886–889.
36. **Powers, R., G. M. Clore, A. Bax, D. S. Garrett, S. J. Stahl, P. T. Wingfield, and A. M. Gronenborn.** 1991. Secondary structure of the ribonuclease H domain of the human immunodeficiency

virus reverse transcriptase in solution using three-dimensional double and triple resonance heteronuclear magnetic resonance spectroscopy. J. Mol. Biol. **221:**1081–1090.

37. **Powers, R., G. M. Clore, S. J. Stahl, P. T. Wingfield, and A. Gronenborn.** 1992. Analysis of the backbone dynamics of the ribonuclease H domain of the human immunodeficiency virus reverse transcriptase using 15N relaxation measurements. Biochemistry **31:**9150–9157.
38. **Prasad, V. R., and S. P. Goff.** 1989. Linker insertion mutagenesis of the human immunodeficiency virus reverse transcriptase expressed in bacteria: definition of the minimal polymerase domain. Proc. Natl. Acad. Sci. USA **86:**3104–3108.
39. **Pullen, K. A., L. K. Ishimoto, and J. J. Champoux.** 1992. Incomplete removal of the RNA primer for minus-strand DNA synthesis by human immunodeficiency virus type 1 reverse transcriptase. J. Virol. **66:**367–373.

39a. **Qiagen Corp.** 1991. Qiagen Manual, p. 26. Qiagen Corp.

40. **Ratner, L., W. Haseltine, R. Patarca, K. J. Livak, B. Starcich, S. F. Josephs, E. R. Doran, J. A. Rafalski, E. A. Whitehorn, K. Baumeister, L. Ivanoff, S. F. Petteway, Jr., M. L. Pearson, J. A. Lautenberger, T. S. Papas, J. Ghrayeb, N. T. Chang, R. C. Gallo, and F. Wong-Staal.** 1985. Complete nucleotide sequence of the AIDS virus, HTLV-III. Nature (London) **313:**277–284.
41. **Restle, T., B. Muller, and R. S. Goody.** 1990. Dimerization of human immunodeficiency virus type 1 reverse transcriptase. J. Biol. Chem. **265:**8986–8988.
42. **Restle, T., B. Muller, and R. S. Goody.** 1992. RNase H activity of HIV reverse transcriptase is confined exclusively to the dimeric forms. FEBS Lett. **300:**97–100.
43. **Restle, T., M. Pawlita, G. Sckakiel, B. Muller, and R. S. Goody.** 1992. Structure-function relationships of HIV-1 reverse transcriptase using monoclonal antibodies. J. Biol. Chem. **267:** 14654–14661.
44. **Roth, M. J., N. Tanese, and S. P. Goff.** 1985. Purification and characterization of murine retroviral reverse transcriptase expressed in *Escherichia coli*. J. Biol. Chem. **260:**9326–9335.
45. **Salazar, M., J. J. Champoux, and B. R. Reid.** 1993. Sugar conformations at hybrid duplex junctions in HIV-1 and Okazaki fragments. Biochemistry **32:**739–744.
46. **Schatz, O., F. V. Cromme, F. Gruninger-Leitch, and S. F. J. Le Grice.** 1989. Point mutations in conserved amino acid residues within the C-terminal domain of HIV-1 reverse transcriptase specifically repress RNase H function. FEBS Lett. **257:**311–314.
47. **Smith, J. S., S. Kim, and M. J. Roth.** 1990. Analysis of long terminal repeat circle junctions of human immunodeficiency virus type 1. J. Virol. **64:**6286–6290.
48. **Smith, J. S., and M. J. Roth.** 1992. Specificity of human immunodeficiency virus-1 reverse transcriptase-associated ribonuclease H in removal of the minus-strand primer, $tRNA^{Lys3}$. J. Biol. Chem. **267:**15071–15079.
49. **Stammers, D. K., M. Tisdale, S. Court, V. Parmar, C. Bradley, and C. K. Ross.** 1991. Rapid purification and characterisation of HIV-1 reverse transcriptase and RNaseH engineered to incorporate a C-terminal tripeptide α-tubulin epitope. FEBS Lett. **283:**298–302.
50. **Starnes, M. C., and Y. Cheng.** 1989. Human immunodeficiency virus reverse transcriptase-associated RNase H activity. J. Biol. Chem. **264:**7073–7077.
51. **Szilvay, A. M., S. Nornes, I. R. Haugan, L. Olsen, V. R. Prasad, C. Endresen, S. P. Goff, and D. E. Helland.** 1992. Epitope mapping of HIV-1 reverse transcriptase with monoclonal antibodies that inhibit polymerase and RNase H activities. J. Acquired Immune Defic. Syndr. **5:**647–657.
52. **Tan, C., J. Zhang, Z. Li, W. G. Tarpley, K. M. Downey, and A. G. So.** 1991. Functional characterization of RNA-dependent DNA polymerase and RNase H activities of a recombinant HIV reverse transcriptase. Biochemistry **30:**2651–2655.
53. **Tanese, N., and S. P. Goff.** 1988. Domain structure of Moloney murine leukemia virus reverse transcriptase: mutational analysis and separate expression of the DNA polymerase and RNase H activities. Proc. Natl. Acad. Sci. USA **85:**1777–1781.
54. **Varmus, H., and P. Brown.** 1989. Retroviruses, p. 53–108. *In* M. H. Howe and D. E. Berg (ed.), Mobile DNA. American Society for Microbiology, Washington, D.C.
55. **Varmus, H. E., and Swanstrom, R.** 1982. Replication of retroviruses, p. 75–134. *In* R. Weiss, N. Teich, H. Varmus, and J. Coffin (ed.), RNA tumor viruses, vol. 1. Cold Spring Harbor Laboratory, Cold Spring Harbor, N.Y.
56. **Whitcomb, J. M., and S. H. Hughes.** 1992. Retroviral reverse transcription and integration: progress and problems. Annu. Rev. Cell Biol. **8:**275–306.
57. **Whitcomb, J. M., R. Kumar, and S. H. Hughes.** 1990. Sequence of the circle junction of human immunodeficiency virus type 1: implications for reverse transcription and integration. J. Virol. **64:**4903–4906.
58. **Worhl, B. M., and K. Moelling.** 1990. Interaction of HIV-1 ribonuclease H with polypurine tract containing RNA-DNA hybrids. Biochemistry **29:**10141–10147.
59. **Wohrl, B. M., S. Volkmann, and K. Moelling.** 1991. Mutations of a conserved residue within HIV-1 ribonuclease H affect its exo- and endonuclease activities. J. Mol. Biol. **220:**801–818.
60. **Yang, W., W. A. Hendrickson, R. J. Crouch, and Y. Satow.** 1990. Structure of ribonuclease H phased at 2A resolution by MAD analysis of the selenomethionyl protein. Science **249:** 1398–1405.